VELOCITY DISPERSIONS AND CLUSTER PROPERTIES IN THE SOUTHERN ABELL REDSHIFT SURVEY CLUSTERS. II.[1]

Hernán Muriel,[2,3] Hernán Quintana,[4] Leopoldo Infante,[4] Diego G. Lambas[2,3] and Michael J. Way[4,5]

ABSTRACT

We report an analysis of the dynamical structure of clusters of galaxies from a survey of photometric and spectroscopic observations in the fields of southern Abell clusters. We analyze the galaxy velocity field in extended regions up to $7\ h^{-1}$ Mpc from cluster centers, and we estimate mean velocity dispersions and their radial dependence. Only one from a total of 41 Abell clusters does not correspond to a dynamically bound system. However, four of these bound objects are double clusters. We estimate that 20% (seven clusters) of the 35 remaining are subject to serious projection effects. Normalizing the clustercentric distances by means of the overdensity radius r_{200}, and the velocity dispersion profiles (VDPs) by the corresponding mean cluster velocity dispersion, we computed the average VDP. Our results indicate a flat behavior of the mean VDP at large distances from the cluster center. Nevertheless, we found that for the inner part of the clusters ($r/r_{200} \leq 1$) the VDP is up to 10% smaller than at larger radii.

Key words: galaxies: clusters: general — galaxies: distances and redshifts — surveys

1. INTRODUCTION

Analysis of large-scale structure formation may greatly benefit from studies of the dynamics of clusters of galaxies. Measurements of galaxy velocity dispersions in clusters provide reliable estimates of cluster masses and a direct normalization of the primordial mass power spectrum (Eke, Cole, & Frenk 1996). Moreover, the velocity field in the extended halos of clusters may set additional important constraints on the formation of structure, as well as on the mean density parameter of the universe.

There have been several recent studies on the dynamics of clusters of galaxies; see, for instance, Girardi et al. (1993), Zabludoff, Franx, & Geller (1993), Collins et al. (1995), Mazure et al. (1996), Fadda et al. (1996), and Alonso et al. (1999). The resulting distribution function of velocity dispersions from the ESO Nearby Abell Cluster Survey (ENACS) given by Mazure et al. (1996) is in agreement with the distribution of cluster X-ray temperatures, suggesting $\beta = \sigma \mu m_h / k T_X \simeq 1$. The velocity dispersion profiles (VDPs) may provide a useful tool for the study of the dynamics of clusters of galaxies. The analysis by Fadda et al. (1996) is consistent with a tendency toward flat VDPs in rich Abell clusters. Jing & Börner (1996) investigated the VDPs of clusters for several cosmological models. They found that on average VDPs decrease with the cluster radius in every model up to $1\ h^{-1}$ Mpc from the cluster center. Also, these authors found that the slope of the profiles is different in different models, being steeper in lower Ω models than in higher Ω models.

In the hierarchical scenario of structure formation, galaxy systems grow by aggregation of smaller structures formed earlier. Therefore, we expect a significant degree of substructure in clusters of galaxies if the remnants of the accretion of groups in the recent past has not been erased by the dynamical relaxation of the clusters. The substructure in rich clusters has been extensively analyzed in recent years (Dressler & Shectman 1988; West & Bothun 1990; Zabludoff et al. 1993; Girardi et al. 1997; Solanes, Salvador-Solé, & Gonzáles-Casado 1999). The results are consistent with substructure in most of the cases studied, irrespective of the samples and method of analyses used. West & Bothun (1990) made an analysis of substructure in clusters of galaxies and their surroundings. The authors developed a technique that is sensitive to correlations between galaxy positions and local kinematics, finding little evidence for substructure in the inner regions and significant departures from a relaxed substructure-free system in the external regions. More recently, Biviano et al. (2002) realized a detailed analysis of the consequences of substructure on luminosity and morphological segregation. These authors find that the number of galaxies in substructures decreases markedly toward the cluster center and report differences in the properties of galaxies depending on whether they belong to substructures or not. These differences are also present in the dynamical properties of galaxies.

Escalera et al. (1994) provide an extensive discussion of the presence of substructure in clusters of galaxies by using galaxy positions and redshifts. In their studies a multiscale analysis is adopted that considers the kinematics, as well as the wavelet transform, providing estimators of the degree of substructure. Other works (see, for instance, Fadda et al. 1996) consider velocity gradients and anisotropy of galaxy orbits. Extensions of the different methods of analysis can provide new useful quantitative estimates of substructure, essential for a better understanding of the dynamics of clusters of galaxies.

The dynamics of clusters of galaxies may also be studied using information in the X-ray band. X-ray emission detected in a large fraction of clusters of galaxies provides

---

an invaluable observational material. Several properties of the clusters and the intracluster medium may be addressed with this information, for example, the global mass distribution, the dynamical state, the evolution with redshift, and the composition of the intracluster medium. White (2000) presents an elegant methodology to recover the spatial properties of the intracluster gas from X-ray observations. From the deconvolution of *ASCA* satellite X-ray data, he finds a large fraction (90%) of clusters consistent with isothermality. These results are in conflict with the Markevitch et al. (1998) analysis of a sample of 30 clusters in which most show steeply declining intracluster temperature profiles. In their analysis of *ASCA*-resolved spectroscopic data these authors obtained projected temperature profiles and in many cases two-dimensional temperature maps, concluding that the gas temperature varies by a factor 1.3–2 or greater within the clusters.

The conflicting evidence for isothermality of the intracluster medium shows that the information on the VDP for clusters may add important information about the subject. On the other hand, the tendency for subclustering to occur at large distances from cluster centers encourages us to explore the outer regions of clusters of galaxies. In this paper, we analyze the radial velocity distribution in regions extending up to $7\,h^{-1}$ Mpc in projection from the Abell cluster center (we adopt $H_0 = 100\,h$ km s^{-1} and $q_0 = 0.5$). We provide a detailed analysis of each individual cluster, providing the degree of substructure and an estimate of the VDP at large distances from the cluster center. In § 3 we describe the method of analysis of substructure. Section 4 deals with the identification of the clusters and the projection effects, which significantly affect the measurements of velocity dispersions. Section 5 provides the estimates of mean velocity dispersion and the correlation with richness counts, as well as the velocity dispersion profile of several clusters.

2. DATA

The SARS survey (Southern Abell clusters Redshift Survey; Way et al. 2002) comprises Abell 1958 and Abell, Corwin, & Ollowin (1989, hereafter ACO) clusters with $R \geq 1$, principally in the regions $0 \geq \delta \geq -65$ and $21 \leq \alpha \leq 24$ and $0 \leq \alpha$ 5 (avoiding the Large and Small and Megallanic Clouds), with $b \leq -40$. Galaxies were selected from the APM catalog (Maddox el al. 1990). Galaxies brighter than $m_R = 19$ and with surface brightness within $1°5 \times 1°5$ centered on the cluster were preselected. Target galaxies were selected at random, and the final completeness is roughly constant up to an apparent magnitude $\sim$18 and it is of the order of 75%.

The observations were carried out with the 2.5 m DuPont telescope at the Las Campanas Observatory, Chile. The multifiber spectrograph (Shectman 1989) was used. Fibers are connected to a Boller & Chivens spectrograph attached to a 2D-Frutti detector. The unknown spectra were calibrated using software packages within IRAF, following essentially the method described by Way, Quintana, & Infante (1997).

From the wavelength-calibrated spectra, the respective radial velocities cz of the unknown spectra were obtained by using two different independent methods: (1) the Fourier cross-correlation technique, in which two Fourier-transformed spectra, the unknown object and a known tem-

plate, are multiplied together to obtain the Fourier transform of their correlation function (with RVSAO; Tonry et al. 1979), and (2) identification of absorption lines " by eye " and computation of cz with the task RVIDLINES. The final sample consists of more than 4000 galaxies with redshift estimates in 41 clusters. Cluster redshifts run from 0.06 to 0.16 with a mean around 0.088.

3. ALGORITHM FOR SUBSTRUCTURE DETECTION

We have applied two different techniques to detect substructure in clusters. These techniques are complementary in the sense that they are mainly designed to remove large structures along the line of sight and smaller systems in three dimensions. Many clusters present double structures in the redshift distribution (e.g., late stage of a cluster-cluster merger). Ashman, Bird, & Zepf (1994) discuss a statistical technique for detecting and quantifying bimodality known as mixture modeling or the KMM algorithm. The scheme is based on applying to the data algorithms that fit a certain number of substructures in redshift space, and the best-fitting model is determined. This technique is the base of commonly adopted procedures used to analyze astronomical data sets, and it assesses the statistical significance of bimodality, providing objective ways of dividing the data into subpopulations. As discussed by Ashman et al. (1994) the KMM technique has broad applicability in the analysis of astronomical data. We have applied this technique to the redshift distribution regardless of the angular position of the galaxies in the field of the cluster. Based on a preliminary inspection of the data, we propose a number of structures with their corresponding mean radial velocities and velocity dispersion that approximately represent the redshift distribution around the cluster. This procedure is restricted to only those structures with overlapping redshift distributions. Then we apply the KMM algorithm and consider a multiple-peak structure when the confidence level for the proposed model is bigger than 90% (for details see Ashman et al. 1994). We have considered different possibilities: (1) when the proposed model for multiple-peak structure is rejected, we consider that the redshift distribution corresponds to a single cluster; (2) if the confidence level of the proposed model is bigger than 90% and at least 70% of the galaxies belong to the same structure, we assume a single cluster and discard the outlying groups, which will deserve a detailed study in a future work; and (3) when most of the galaxies belong to two separate structures of similar sizes, we assume the presence of two clusters and perform the corresponding analysis. It should be noted that the above technique works properly when the substructures are representative of a significant number of galaxies. In this work only structures with at least 10 galaxies are considered.

In the hierarchical model for large-scale structure formation, clusters of galaxies are the result of a continuous process of accretion of small structures such as groups of galaxies. Therefore, a considerable number of galaxies are expected to be found around clusters that are not bound to the main system and therefore will bias the velocity dispersion estimate if they are included in the analysis. This problem is particularly serious if large distances from the cluster center are considered, as is the case in the present work. Some of these groups of galaxies can be located at a redshift

similar to that of the cluster; therefore, they are very difficult to detect in the redshift space.

In our data set and for each cluster we analyze the real nature of visually identified group candidates with a technique that considers both the projected position and redshift of the galaxies by using the compactness of the projected distribution and the departure from the mean dynamical properties of the cluster. Three different parameters are used: (1) a δ parameter similar to that defined by Dressler & Shectman 1988,

$$\delta^2 = (11/\sigma^2)[(v_{\rm loc} - v)^2 + (\sigma_{\rm loc} - \sigma)^2] ,$$

where σ and $\sigma_{\rm loc}$ are the velocity dispersion of the cluster and the proposed group structure, respectively, and v and $v_{\rm loc}$ are the corresponding mean velocities; (2) a parameter C, which provides a measure of the compactness of groups and is computed as $C = \langle {\rm dnn}_{\rm loc} \rangle / \langle {\rm dnn}_{\rm grp} \rangle$, where $\langle {\rm dnn}_{\rm grp} \rangle$ is the average projected distance of the nearest neighbors to each of the nearest galaxy members of the proposed group and $\langle {\rm dnn}_{\rm loc} \rangle$ is computed in the same way but for the nearest galaxies in the neighborhood of the proposed group; and (3) an isolation parameter $I = {\rm dnng}/\langle {\rm dnn}_{\rm grp} \rangle$, where dnng is the distance to the nearest neighbor galaxy to the group.

We compute the variable $G = \delta + C + I$, and we calculate the mean $\langle G \rangle$ and the dispersion σ_G for each cluster. A given group candidate is to be removed if the value of G for the group is at least two standard deviations, $2\sigma_G$, away from the cluster mean value $\langle G \rangle$. The adopted threshold is the result of Monte Carlo simulations, which show that this threshold is suitable to remove structures. For the five most regular clusters in our sample we reassigned the polar angle of every galaxy with respect to the cluster center. This procedure removes group structures and leaves unchanged the radial galaxy density profile of the cluster. For the mock data, we compute G, identifying mock groups of galaxies and finding that none of these chance groups have $G - \langle G \rangle \geq 2\sigma_G$ (with $\langle G \rangle$ and σ_G computed from the original data).

In spite of the fact that our sample of galaxies in clusters is not magnitude limited the above procedure should give no biased results provided the galaxies are randomly selected from a complete sample.

4. ANALYSIS

As a result of the two techniques described above we have removed 19 structures in 14 clusters from our total sample of 41 Abell clusters. We find that four Abell clusters appear as two different systems in redshift space, and one Abell cluster is completely spurious. In the following sections we discuss different properties of the resulting 44 clusters. Table 1 shows the Abell number, the total number of galaxies with measured redshift in the line of sight to the cluster ($N_{\rm tot}$), the number of galaxies assigned to the cluster ($N_{\rm clu}$), and the cluster mean radial velocities.

4.1. *Cluster Identification*

In our analysis we have considered only clusters selected by Abell (1958) and ACO. Several authors (van Haarlem, Frenk, & White 1997 and references therein) have discussed the consequences of the projection effects when clusters are selected from a two-dimensional catalog. Redshift surveys provide precise information on the reality of the clusters

TABLE 1
CLUSTER SAMPLE AND NEW MEAN VELOCITIES AND DISPERSIONS

Abell Number	$N_{\rm tot}$	$N_{\rm clu}$	$\langle {\rm Vel} \rangle$ (km s^{-1})	σ (km s^{-1})
80	109	45	19013 ± 48	322 ± 52
118	38	19	34421 ± 159	669 ± 127
380	110	20	31997 ± 161	697 ± 102
487	87	15	34354 ± 84	309 ± 57
1271	53	10	51019 ± 219	640 ± 132
1750	60	23	25089 ± 102	477 ± 66
2734	105	62	18502 ± 100	784 ± 124
2778	49	17	31125 ± 215	$[852 \pm 143]$
2799	49	21	19454 ± 127	563 ± 62
2800	130	51	18943 ± 47	335 ± 64
2819a	48	12	22306 ± 147	477 ± 140
2819b	...	13	25917 ± 80	272 ± 54
2854	119	37	18480 ± 51	308 ± 44
2871a	109	24	34122 ± 64	317 ± 75
2871b	...	23	36463 ± 68	319 ± 67
2911	134	41	24049 ± 86	546 ± 97
2915	105	18	25713 ± 55	224 ± 136
2923	111	26	21420 ± 135	670 ± 76
2933	97	53	27709 ± 105	759 ± 72
3107a	78	19	19463 ± 148	623 ± 114
3107b	...	12	23201 ± 168	544 ± 102
3111	111	48	22891 ± 121	827 ± 77
3112	108	49	22679 ± 92	637 ± 63
3122	90	47	19048 ± 121	819 ± 98
3135	111	53	18733 ± 81	585 ± 57
3141	98	40	30923 ± 73	454 ± 87
3142	111	46	31041 ± 171	1145 ± 163
3151	107	28	20812 ± 64	330 ± 44
3152	57	10	28478 ± 138	403 ± 102
3153	91	21	37068 ± 157	$[698 \pm 149]$
3159	71	...	...	...
3188	53	15	19123 ± 129	474 ± 224
3189	87	23	18071 ± 49	228 ± 47
3194	97	48	29103 ± 91	625 ± 70
3223a	205	73	17920 ± 80	684 ± 64
3223b	...	41	17904 ± 64	407 ± 57
3264	95	39	29338 ± 114	704 ± 66
3764	115	53	22714 ± 110	795 ± 123
3809	89	49	18785 ± 81	560 ± 67
3844	102	19	43735 ± 90	379 ± 42
3864	99	29	30699 ± 161	847 ± 188
3915	85	61	28925 ± 105	815 ± 102
3921	94	57	27855 ± 105	788 ± 111
4010	28	26	28766 ± 149	743 ± 140
4067	50	18	29643 ± 181	738 ± 442

selected. As a result of our analysis we found only one spurious cluster (Abell 3159) while the rest appear as real concentrations in redshift space. Nevertheless, 11 clusters present more than one concentration in the redshift space, thus in projection they appear as richer clusters. Of the total of 40 Abell clusters 28 appear as a single concentration in the total redshift range, while the rest have been systematically enhanced by projection effects. We consider that a cluster is significantly affected by projections when the number of galaxies in groups or other cluster-like structures along the line of sight is comparable to the number of confirmed cluster members. Besides the projection effects, after the removal of structures previously described several clusters present significant evidence for substructure on different levels. This substructure can affect the analysis of the dynamics of clus-
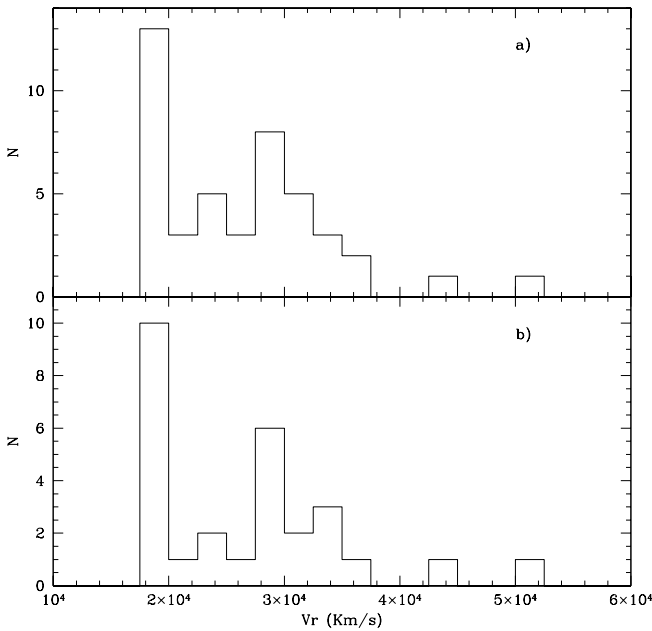
Fig. 1.—Histogram of mean radial velocities of the clusters: (*a*) the total sample, (*b*) relaxed clusters.

ters. In particular, the estimate of the velocity dispersion may be significantly affected by substructure.

We will use the term " relaxed cluster " to describe a system that is free from substructure with a single nearly Gaussian redshift distribution after the subtraction of structures by using the procedure discussed in § 3. This classification will be used to define subsamples of clusters. Our original cluster sample is not volume-complete, and the above definition is used to select subsets of clusters to cross-correlate general properties such as richness counts, mean velocity dispersions, etc. Figure 1*a*–1*b* shows, respectively, the mean redshift distribution of the total sample clusters and those classified as relaxed; the similarity of the mean radial velocity distributions can be appreciated.

4.2. *Substructure Properties*

We have analyzed the properties of the different structures removed from clusters. As a result of the algorithm of group detection we find an average velocity dispersion $\sigma_g = 295 \pm 180$ km s^{-1} and a mean extension $D = 0.44 \pm 0.28 \, h^{-1}$ Mpc. These structures, which compose 12% of the total number of galaxies in the clusters, have on average a difference of mean velocity with respect to the parent cluster $\Delta V = 921 \pm 393$ km s^{-1}. Our values of σ and D are typical of groups of galaxies. Nevertheless, the average extensions of our groups are larger than those derived by Girardi et al. 1997 ($\sim 0.2 \, h^{-1}$ Mpc). The KMM technique for substructure detection tends to identify systems at larger distances from the cluster center ($\Delta V = 1515 \pm 304$ km s^{-1}). Nevertheless, the mean velocity dispersion of these structures (288 ± 128 km s^{-1}) is similar to the σ_g derived by the group detection algorithm.

4.3. *Individual Objects*

Several clusters in our analysis deserve individual attention because of peculiarities of their properties.

The redshift distribution along the line of sight to A2819, A2871, A3107, and A3223 shows two similar structures not physically connected. In Table 1 each of these clusters is identified by the original Abell number with an " a " or " b," respectively.

As an example of the application of the method we comment on the cluster A2734, which presents a double-peaked structure in redshift space. The smallest peak has approximately half the number of members of the main structure. It was removed since the probability of two different structures is 99%.

A380 presents some evidence of a double structure with a mean velocity difference of 1407 km s^{-1}. The probability of two different structures is larger than 90%. Nevertheless, the low number of galaxies (25) involved in our analysis introduces some doubts about our conclusions. The values quoted in Table 1 correspond to a single cluster. Assuming two different structures, we find the following values: $\langle V \rangle = 31,440$ km s^{-1}, $\sigma = 408$ for the nearest structure (14 galaxies) and $\langle V \rangle = 32,847$ km s^{-1}, $\sigma = 314$ for the second (11 members).

Besides the clusters that appear to be double in the redshift space, A380, A487, A2915, A3142, A3153, A3844, and A3864 present strong projection effects due to the presence of several structures such as groups of galaxies along the line of sight.

A3111: This cluster shows some evidence of large-scale substructures in the plane of the sky. Our algorithm does not work properly for this type of substructure; therefore, the cluster was taken as a single structure, and the value quoted in Table 1 (827 km s^{-1}) could be biased upward. Nevertheless, the discrepancy with the velocity dispersion derived by Fadda et al. 1996 (159 km s^{-1}) cannot be explained. If we arbitrarily restrict ourselves to the central region of the cluster (up to 2.5 Mpc h^{-1} in diameter), where no evidence of substructure is present, we derive $\sigma = 734$ km s^{-1}. This value must be taken as a lower limit for the mean velocity dispersion of A3111. The value derived by Fadda et al. (1996) is probably biased by the low number of confirmed members in their sample (12 galaxies) while our analysis is based on more than 50 cluster members.

A3151: This cluster presents a group of galaxies in its very center with a mean velocity differing by more than 900 km s^{-1} with respect to the main cluster. This is nearly the same difference between our estimate of the cluster mean velocity and the value derived by Fadda et al. 1996. Their estimate is the result of 14 galaxies, and by chance they selected galaxies from the projected group instead of the main cluster.

A3223: In the plane of the sky A3223 appears as two separate structures and hence was treated as two different clusters. These two clusters also show important differences in their dynamical properties. The second concentration was identified by the APM selection criteria and is named APMCC 479.

A1750, A3111, A3135, A3764, and A3915: After the removal of groups and in addition to those indicating double structures, A1750, A3111, A3135, A3764, and A3915 still present some evidence for substructure in redshift space or in the plane of the sky.

A3159: The redshift distribution in the line of sight of this cluster shows the presence of several groups; nevertheless, none of these groups can be classified as a cluster. We suggest this system is a spurious cluster identification.

A2778 and A3153: These are two clusters poorly defined both in the plane of the sky and in redshift space, where the presence of gaps suggests the possibility of substructure. More redshifts are needed to clearly understand these clusters. The values of σ quoted in Table 1 for these two clusters must be taken with caution, especially in the case of A3153, for which the redshift distribution can also be consistent with several groups instead of a single cluster.

5. VELOCITY DISPERSION ESTIMATES

After the redefinition of structures as defined in § 3 we have computed the mean velocity dispersion for each cluster. Based on the ROSTAT routine (see Beers, Flynn, & Gebhardt 1990) we have used robust mean and scale estimators. We have applied relativistic corrections and have taken into account velocity errors. Considering the typical number of redshift-confirmed cluster members (usually >20) we have considered the *biweight* estimate for both the mean cluster radial velocity and the velocity dispersion. Errors are based on the statistical *jacknife*. The derived values are shown in Table 1. Figure 2a shows the values of the mean velocity dispersion for clusters in the range 200–1100 km s^{-1} with a mean $\approx$600 km s^{-1}, indicating that in our study we have included low-mass systems (probably groups), as well as massive clusters of galaxies. Figure 2b shows the same distribution but only for those clusters classified as relaxed. That no differences between both sets of data are present can be appreciated, indicating that contamination by projection effects is seen at some degree in all clusters, irrespective of redshift and σ.

5.1. Comparison with Other Estimates

Twenty of the clusters in our sample are also in the ENACS survey. Figure 3a shows the comparison between our estimates and those obtained by Fadda et al. 1996.
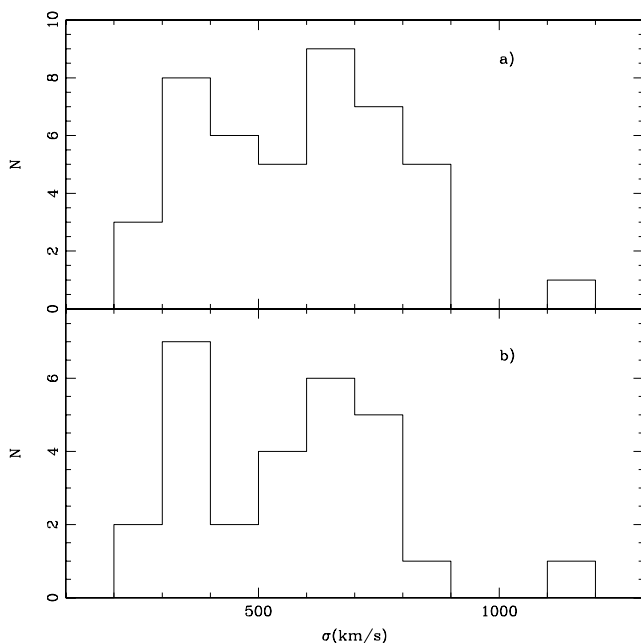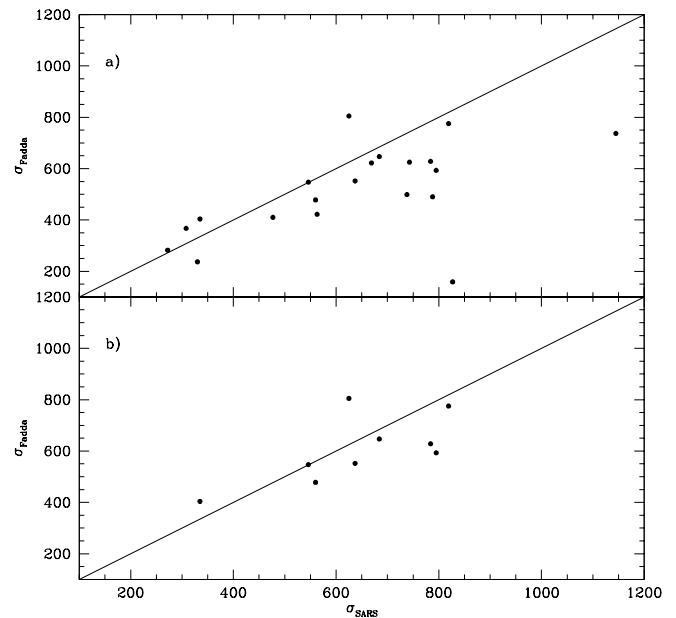

Fig. 3.—(a) Comparison with Fadda et al. 1996 results. The solid line corresponds to equal σ. (b) Same as (a) but for clusters with at least 30 confirmed members in both samples. The solid line corresponds to equal σ.

We found a mean difference $\langle \sigma_{\mathrm{Fad}} - \sigma_{\mathrm{SARS}} \rangle = -89 \pm 132$, which indicates that our values of σ are on average slightly higher than those of Fadda et al. (1996). If we restrict our sample to those clusters with at least 30 confirmed members (the same restriction is applied in Fadda et al. 1996) we find $\langle \sigma_{\mathrm{Fad}} - \sigma_{\mathrm{SARS}} \rangle = -40 \pm 108$, which suggests a smaller shift and spread (see Fig. 3b). In both cases we have made the comparison assuming the same cluster radius as Fadda et al. 1996 (typically smaller than our maximum cluster radii).

Fig. 2.—Histogram of mean velocity dispersion of the clusters: (a) the total sample, (b) relaxed clusters.
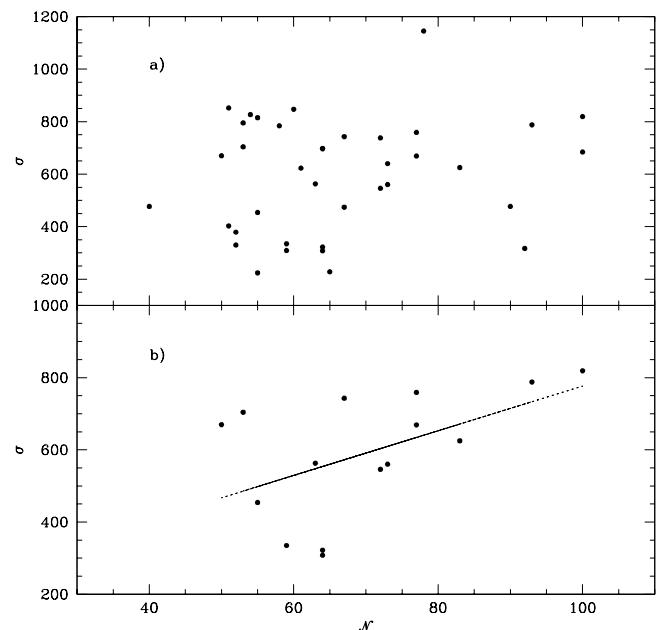

Fig. 4.—(a) Correlation between the mean velocity dispersion estimate and the richness counts estimated by ACO. (b) Same as (a) but for relaxed clusters.

5.2. *Cluster Mean Velocity Dispersion versus Richness Counts*

Taking into account the methods previously described, we have computed the mean velocity dispersions for our sample of clusters. We have performed a comparison between σ and the richness number counts N as defined in the ACO catalog. Since only a small fraction of our cluster sample consists of known X-ray emitters, we have not attempted to analyze correlations between our dynamical estimates and the X-ray information.

Figure 4a, in which no clear correlation can be appreciated, shows the correlation between σ and the richness counts N taken from the ACO catalog. A similar result was found by Mazure et al. (1996). These authors suggest that the very broad relation between N and σ must be largely intrinsic. Nevertheless, when we restrict the sample to the relaxed clusters and "isothermal" distributions (Gaussian velocity distribution and flat or slowly decaying VDP; see the next section for details) and exclude those clusters more strongly affected by projection effects, the data suggest some correlation between richness counts and σ in the sense that the richest clusters tend to have higher σ. This correlation can be seen in Figure 4b, where a linear fit has been applied, deriving the following relation: $\sigma = (6.2 \pm 2.8)N + (158 \pm 202)$.

5.3. *Velocity Dispersion Profiles*

The large projected area around clusters in the SARS survey allows us to analyze the dynamics of galaxies in the extended halos of clusters. A useful statistical measure of the dynamics is the velocity dispersion profile, the velocity dispersion at a given radius evaluated by using all the galaxies within that radius. The VDP was computed for the 29 clusters in our sample with more than 20 confirmed mem-
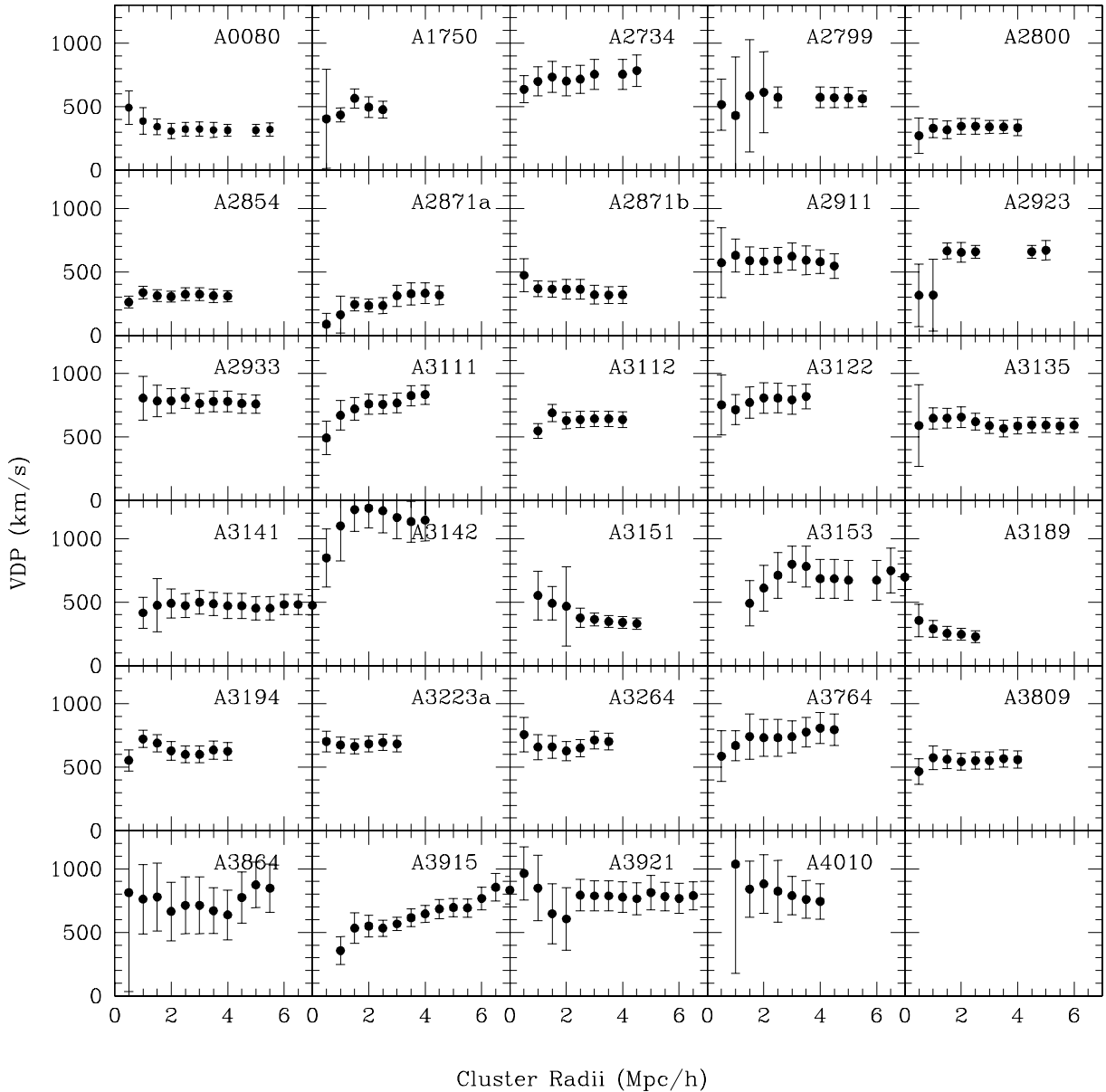

Fig. 5.—Velocity dispersion profiles for 29 Abell clusters

bers. We have used a step size of 0.5 Mpc h^{-1} while most VDPs are computed up to 4 Mpc h^{-1} and in some cases beyond this radius. Many clusters show an irregular trend in the inner part (cluster radius ≤ 1 Mpc h^{-1}); this effect could be weakly related to the low number of galaxies in the inner part of the cluster and may also depend on the choice of the cluster center, which in our case corresponds to the values provided by Abell. Nevertheless, the most interesting
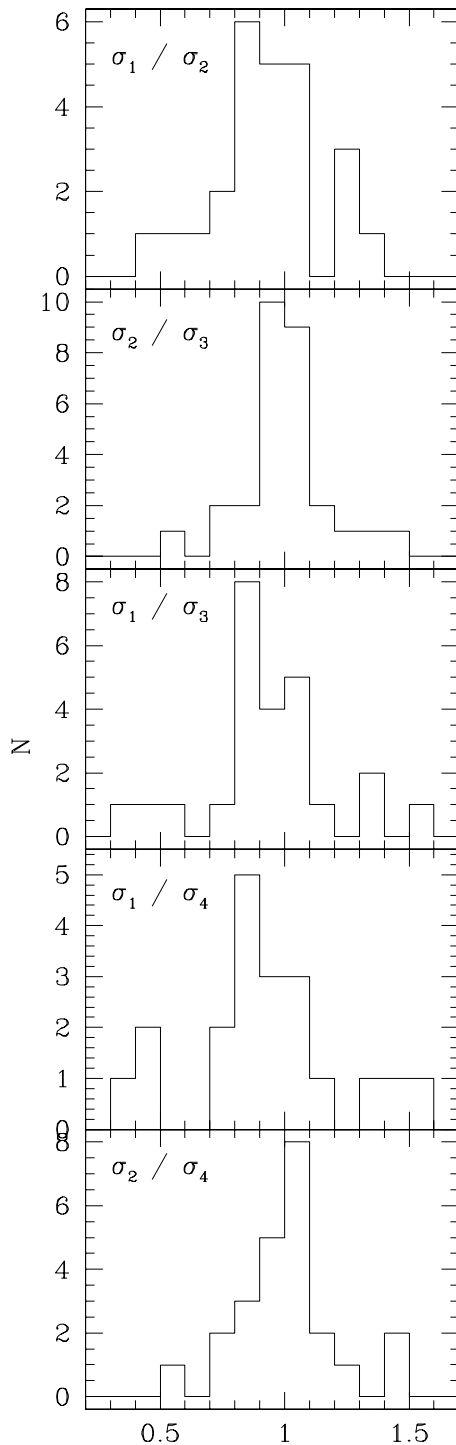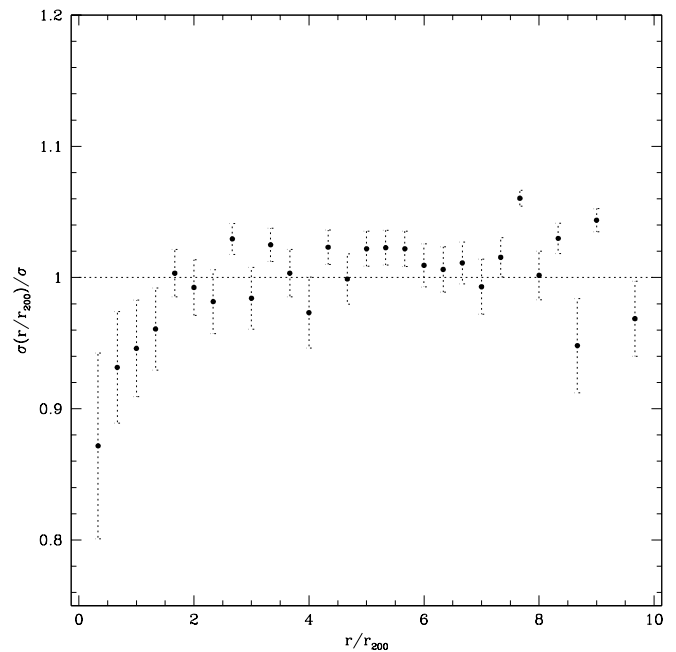

FIG. 7.—Mean VDP for the total sample of clusters with VDP estimates. Each cluster has been normalized using the corresponding mean σ.

aspect of the VDPs is their behavior at large distances from the cluster center. For these 29 clusters we find 19 (14 are relaxed clusters) with a flat VDP, five with a slowly decaying profile, and five with a rising profile. It should be noted that only one of the VDP rising clusters was classified as a relaxed cluster. These results are shown in Figure 5 for the 29 objects with reliable estimates of VDP.

To allow for a physical comparison between clusters with different mean velocity dispersions, we have normalized the cluster radii by using r_{200} (the radius for which the mean interior cluster overdensity is 200). Assuming a singular isothermal profile Carlberg, Yee, & Ellingson (1997) derive the following correlation between r_{200} and the cluster mean velocity dispersion: $r_{200} = 3^{1/3}\sigma/10$ $H_0(z)$. We have followed an analysis similar to that proposed by den Hartog & Katgert (1996) and Jing & Börner (1996), consisting of the computation of the ratios of σ at different distances from the cluster center. Both den Hartog & Katgert (1996) and Jing & Börner (1996) use the radius in megaparsecs (up to 3 and 1 Mpc h^{-1}, respectively). We propose the use of a normalized radius and four bins for the computation of the velocity dispersion estimates σ_1, σ_2, σ_3, and σ_4: $r/r_{200} < 1$, $r/r_{200} < 2$, $r/r_{200} < 3$, and $r/r_{200} \leq 7$, respectively. The shape of the VDP at different radii can be quantified by the ratios σ_i/σ_j (=1 for a flat profile). In Figure 6 we show the distribution of the following ratios: σ_1/σ_2, σ_2/σ_3, σ_1/σ_3, σ_1/σ_4, and σ_2/σ_4, and the derived mean values are 0.93, 1.00, 0.95, 0.96, and 1.00, respectively. It can be appreciated that those ratios involving σ_1 suggest that in the inner bin (up to $r/r_{200} = 1$) the velocity dispersion is approximately 10% lower than at larger distances. This fact can also be appreciated in Figure 7, where the total sample of clusters has been averaged, each VDP profile being normalized with the corresponding mean cluster velocity dispersion. Figure 7 also clearly shows that the average VDP for $r/r_{200} > 1.5$ is nearly flat well beyond the cluster virial radius.

FIG. 6.—Velocity dispersion ratios between values of σ computed for different normalized bins: σ_1, σ_2, σ_3, and σ_4 correspond to $r/r_{200} < 1$, $r/r_{200} < 2$, $r/r_{200} < 3$, and $r/r_{200} \leq 7$, respectively.

6. DISCUSSION AND CONCLUSIONS

A significant degree of substructure in clusters of galaxies is expected in the hierarchical scenario of structure formation. This is because of the large timescale for the remnants of the accretion of groups onto clusters in the recent past to be erased by dynamical relaxation. On the other hand, the identification of clusters in two dimensions may be strongly biased by spurious systems because of projection effects as shown in numerical simulations (van Haarlem et al. 1997). These two issues heavily complicate a detailed analysis of the dynamical properties of clusters of galaxies.

The evidence for substructure in rich clusters has been extensively explored in different studies of the galaxy distribution in cluster fields for which the most accepted view is the relevant presence of substructure. The X-ray observations also contribute to our knowledge of the spatial properties of the intracluster gas. However, recent analyses provide conflicting results regarding the isothermality of the gas or the existence of steeply declining temperature profiles. This issue and the fact that the degree of substructure increases at large distances from cluster centers motivated the present study of the outer regions of clusters of galaxies. Our work is mainly centered on the analysis of the radial velocity distribution of galaxies in extended regions of Abell clusters, focusing on the existence of gradients in the velocity dispersion profiles.

We have carried out an analysis of the velocity field of galaxies in extended regions up to $7 \ h^{-1}$ Mpc from the cluster centers. We have applied several methods to remove contamination caused by projection effects and analyzed the presence of subclustering. We have obtained suitable estimates of the mean velocity dispersions and its radial dependence by using the ROSTAT routines. Our analysis can be compared with that of Fadda et al. (1996) for a fraction of common objects. It is clear from our analysis that the larger differences arise in those clusters with more contamination and a smaller number of measured redshifts. We also find that the correlation between mean velocity dispersion σ and richness number counts $7 \ h^{-1}$ is strongly affected by projection effects. There is some evidence of correlation between σ and $7 \ h^{-1}$ for a subsample restricted to systems with no significant degree of contamination.

From our original sample of 41 Abell clusters we found that 40 are real clusters although four of these appear to be double systems. These results are similar to those found by Mazure et al. 1996. These authors found that almost all ACO clusters with richness class 1 or greater correspond to real systems in the redshift space and about 10% of the ACO clusters appear to be the result of a superposition of two similar poorer systems. Beside the double systems we also found that seven of the clusters in our sample are subject to serious projection effects. The fraction of clusters with a high degree of contamination in our sample compares well with the results of such effects in the mock catalogs from the numerical simulations of van Haarlem et al. (1997), in which 1/3 of Abell-type clusters are expected to arise from projection of groups along the line of sight.

From the resulting sample of 44 clusters, four are poorly defined and more data are needed to better establish their properties. In spite of projection effects, 28 of the 44 clusters are well defined in redshift space and have a velocity distribution consistent with a Gaussian function.

Our results show that the average VDP is flat at large distances from the cluster center. This behavior is found for 19 clusters (65% of the 29 with VDP estimates), indicating that an isothermal hypothesis can be assumed even at radii well beyond the virial radius. Nevertheless, we found that on average the normalized velocity dispersion is about 10% smaller in the inner region of the clusters ($r/r_{200} \leq 1$). A possible interpretation of the decay of VDPs in central regions can be related to the morphological segregation in clusters. Fadda et al. (1996) found kinematical segregation in the sense that early-type galaxies show smaller values of σ than late types; Mazure et al. (1996) found that the brightest cluster galaxies (typically of early-type morphology) move slower than other galaxies, and Ramírez et al. (1998) found that the differences between the velocity distributions of elliptical and spiral galaxies are associated with the shape of their orbit families. Since early-type objects are dominant within r_{200} the results shown in Figure 7 are to be expected.

The shape of VDP profiles are of fundamental importance for their implications for cluster properties and cosmology since detailed theoretical predictions from different cosmological scenarios could be used to set restrictions to current models of structure formation. The Jing & Börner (1996) analysis of VDPs of clusters for several cosmological models shows an average decline of VDPs with the distance to cluster centers. Nevertheless, this analysis was restricted to the very inner region of the clusters ($\leq 1 \ h^{-1}$ Mpc). Therefore, new numerical simulations must be analyzed to test our findings of flat VDPs at very large distances from the cluster center.

Under the assumption that clusters are in global dynamical equilibrium (even beyond the virialization radius) our results can be compared with temperature radial distributions derived from the X-ray emission of the intracluster medium. Flat VDPs at large clustercentric distances may shed light on the recent controversy on the nature, either flat or declining, of intracluster temperature radial profiles (see White 2000).

REFERENCES

Abell, G. O. 1958, ApJS, 3, 211
Abell, G. O., Corwin, H. G., Jr., & Olowin, R. P. 1989, ApJS, 70, 1 (ACO)
Alonso, M. V., Valotto, C., Lambas, D. G., & Muriel, H. 1999, MNRAS, 308, 618
Ashman, K. M., Bird, C., & Zepf, S. E. 1994, AJ, 108, 2348
Beers, T. C., Flynn, K., & Gebhardt, K. 1990, AJ, 100, 32
Biviano, A., Kathert, P., Thomas, T., & Adami, C. 2002, preprint (astro-ph/0201540)
Carlberg, R. G., Yee, H. K. C., & Ellingson, E. 1997, ApJ, 478, 462
Collins, C. A., Guzzo, L., Nichol, R. C., & Lumsden, S. L. 1995, MNRAS, 274, 1071
den Hartog, R., & Katgert, P. 1996, MNRAS, 279, 349
Dressler, A., & Shectman, S. A. 1988, AJ, 95, 985
Eke, V. R., Cole, S., & Frenk, C. 1996, MNRAS, 282, 263
Escalera, E., Biviano, A., Girardi, M., Giuricin, G., Mardirossian, F., Mazure, A., & Mezzetti, M. 1994, ApJ, 423, 539

Fadda, D., Girardi, M., Giuricin, G., Mardirossian, F., & Mezzetti, M. 1996, ApJ, 473, 670

Girardi, M., Biviano, A., Giuricin, G., Mardirossian, F., & Mezzetti, M. 1993, ApJ, 404, 38

Girardi, M., Escalera, E., Fadda, D., Giuricin, G., Mardirossian, F., & Mezzetti, M. 1997, ApJ, 482, 41

Jing, Y. P., & Börner, G. 1996, MNRAS, 278, 321

Maddox, S. J., Efstathiou, G., Sutherland, W. J., & Loveday, J. 1990, MNRAS, 243, 692

Markevitch, M., Forman, W. R., Sarazin, C. L., & Vikhlinin, A. 1998, ApJ, 503, 77

Mazure, A., et al. 1996, A&A, 310, 31

Ramírez, A., & de Souza, R. E. 1998, ApJ, 496, 693

Shectman, S. 1989, Carnegie Institution of Washington Yearbook (Washington: Carnegie Inst. of Washington), 25

Solanes, J. M., Salvador-Solé, E., & Gonzáles-Casado, G. 1999, A&A, 343, 733

Tonry, J., & Davis, M. 1979, AJ, 84, 1511

van Haarlem, M. P., Frenk, C. S., & White, S. D. 1997, MNRAS, 287, 817

Way, M. J., Quintana, H., & Infante, L. 1997, preprint (astro-ph/9709036)

Way, M. J., Quintana, H., Infante, L., Muriel, H., & Lambas, G. D. 2002, in preparation

West, M. J., & Bothun, G. D. 1990, ApJ, 350, 36

White, D. A. 2000, MNRAS, 312, 663

Zabludoff, A. I., Franx, M., & Geller, M. J. 1993, ApJ, 419, 47